The impact of a shock wave on a movable wall

By R. F. MEYER
Department of the Mechanics of Fluids, University of Manchester

(*Received* 29 *August* 1957)

SUMMARY

An approximate solution is devised for the one-dimensional motion following the impact of a shock wave on a wall which is free to move. The approximate solution neglects changes in entropy occurring through the reflected and transmitted shocks, thus reducing the problem to one of a simple wave type. The asymptotic behaviour of the system is considered and it is shown by exact physical argument that the transmitted shock eventually attains the same strength as the incident shock and that the reflected shock ultimately decays to a sound wave.

An experimental investigation of the interaction was made, using thin walls of cellulose acetate, in a shock tube at an incident shock Mach number of 1·50. Agreement between the theoretical and experimental results, especially for the path followed by the wall, was found to be good.

1. INTRODUCTION

When a wall of small mass, initially at rest and free to move under impact, is struck head-on by a plane shock wave, the resulting difference in pressure between the two sides of the wall causes it to accelerate in the direction of the initial motion of the incident shock wave and thereby to send out compression waves into the region ahead of the wall and rarefaction waves into the region behind it. The compression waves overtake and eventually coalesce to form a shock, whereas the rarefaction waves catch up the reflected shock and weaken it. The appropriate wave diagram, for the interaction is sketched in figure 1, where x and t designate distance and time respectively. Ultimately the pressure difference across the wall vanishes, so that the wall and the transmitted shock attain constant speeds; the reflected shock on the other hand decays to a sound wave.

This paper describes a theoretical and experimental study of the problem, which will be treated as essentially one-dimensional.

The complete analytical problem of determining the motion of the wall, the behaviour of the transmitted shock and the behaviour of the reflected shock, is difficult and not attempted here. Courant & Friedrichs (1948) state, when discussing the strong shock produced by an accelerating piston, that "the problem is an initial boundary value problem with an unknown boundary and that no direct theoretical treatment seems possible". Pillow & Levey (1947) and Pillow (1949) found an analytical solution for the shock

produced by a *uniformly* accelerating piston, which is correct to the first order in entropy changes through the shock. It would seem difficult, however, to extend their method to a problem involving a more general motion of the piston and more difficult still to extend it to the present problem in which the motion of the piston is unknown to start with. Courant & Friedrichs (1948), Friedrichs (1948) and Rudinger (1955) indicate that the problem could be solved numerically by a step-by-step integration by the method of characteristics, but since the motions of the wall, the transmitted shock and the reflected shock are all interdependent such a solution would be lengthy and tedious.

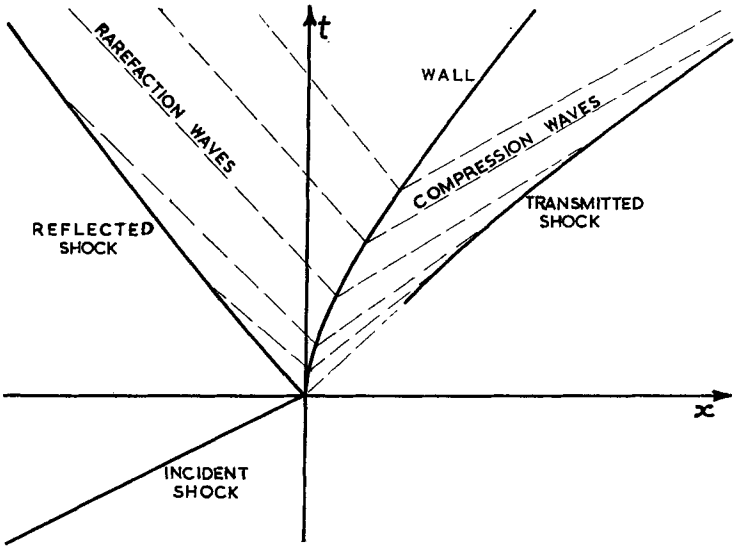

Figure 1. Wave diagram for the motion following the one-dimensional impact of a shock wave on a movable wall.

The theoretical solution given in this paper is approximate. The changes in specific entropy occurring through the transmitted and reflected shocks are neglected, so that the problem reduces to one of a simple wave type in which it is possible to determine the motion of the wall independently of the transmitted and reflected shocks. Having determined the path followed by the wall, the transmitted and reflected shocks are determined by Friedrichs' (1948) theory. Such a theory is accurate to the second order in shock strength and should therefore be reasonably accurate provided that the incident shock is not too strong.

The asymptotic behaviour of the system is considered and is shown to be exactly determinable independently of the approximate theory. Comparison is made, for varying shock Mach numbers, between the asymptotic speed of the wall as determined exactly and as determined by the approximate theory, the difference between the two giving a measure of the accuracy of the approximate theory.

The experimental investigation was made using movable walls of thin cellulose acetate, in a shock tube at an incident Mach number of 1·5. The ideal one-dimensional conditions of the theory could not be reproduced exactly because of the difficulty in avoiding a small amount of leakage past the edges of the wall, but results of the experiment show that the approximation to the one-dimensional problem was quite good, and in particular, that the motion of the wall was, for some time at least, little affected by the small amount of leakage. The agreement between theory and experiment for the path followed by the wall was excellent; for the shocks some discrepancies between theory and experiment were observed which could be attributed, in part at least, to the leakage past the edges of the wall.

2. Theory

The full characteristic equations for the regions between the shocks and the wall are

$$\frac{\partial}{\partial t}\left(\frac{2}{\gamma-1}a\pm u\right)+(u\pm a)\frac{\partial}{\partial x}\left(\frac{2}{\gamma-1}a\pm u\right)=\pm\frac{a^2}{(\gamma-1)c_p}\frac{\partial s}{\partial x}$$

and $Ds/Dt = 0$, where a, u, s are respectively the velocity of sound, particle velocity and specific entropy. If the changes in specific entropy through the transmitted and reflected shocks are neglected, the flow in the regions ahead of and behind the wall is isentropic and the characteristic equations reduce to

$$\frac{\partial}{\partial t}\left(\frac{2}{\gamma-1}a\pm u\right)+(u\pm a)\frac{\partial}{\partial x}\left(\frac{2}{\gamma-1}a\pm u\right)=0.$$

We then have that

$$P=\frac{2}{\gamma-1}a+u=\text{constant along}\ \frac{dx}{dt}=u+a,$$

and

$$Q=\frac{2}{\gamma-1}a-u=\text{constant along}\ \frac{dx}{dt}=u-a.$$

P and Q are the Riemann invariants. Since the change in specific entropy through the transmitted shock is neglected it follows that Q must be constant through the transmitted shock. Q is everywhere constant ahead of the transmitted shock and so must be everywhere constant ahead of the wall. Similarly it may be argued that P is everywhere constant behind the wall. Since Q is constant in the flow region between the wall and the transmitted shock, the positive characteristics (lines along which P is constant) are straight lines along which the flow properties are constant. In other words, the compression waves are simple waves. Similarly the negative characteristics in the region between the wall and the reflected shock are straight lines along which the flow properties are constant.

Consider some general point *ef*, figure 2, on the wall, where *f* refers to the conditions on the leading side of the wall and *e* refers to conditions on the trailing side. Ahead of the wall

$$Q_f=\frac{2}{\gamma-1}a_f-u_f=\text{constant}=Q_1,$$

which, together with the isentropic relation, leads to

$$\frac{p_f}{p_1} = \left(\frac{a_f}{a_1}\right)^{2\gamma/(\gamma-1)} = \left(\frac{Q_1+u_f}{Q_1}\right)^{2\gamma/(\gamma-1)},$$

where p is the pressure and the suffix 1 denotes the uniform initial conditions ahead of the wall.

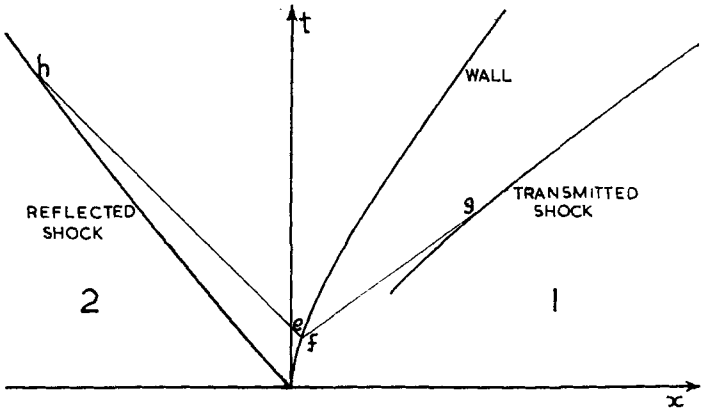

Figure 2. Wave diagram 1 denotes the region of uniform conditions into which the transmitted shock is advancing and 2 denotes the region of uniform conditions into which the reflected shock is advancing.

Similarly we have for the pressure on the trailing side of the wall

$$\frac{p_e}{p_{e0}} = \left(\frac{P_2-u_e}{P_2}\right)^{2\gamma/(\gamma-1)};$$

hence

$$p_e - p_f = p_{e0}\left(\frac{P_2-u_w}{P_2}\right)^{2\gamma/(\gamma-1)} - p_1\left(\frac{Q_1+u_w}{Q_1}\right)^{2\gamma/(\gamma-1)},$$

where the suffix 0 denotes the conditions at $t = 0$, and $u_e = u_f = u_w$. Thus

$$\frac{du_w}{dt} = \frac{p_e-p_f}{p_{e0}-p_1}\left(\frac{du_w}{dt}\right)_{t=0}$$

$$= \left(\frac{du_w}{dt}\right)_{t=0}\frac{p_1}{p_{e0}-p_1}\left[\frac{p_{e0}}{p_1}\left(\frac{P_2-u_w}{P_2}\right)^{2\gamma/(\gamma-1)} - \left(\frac{Q_1+u_w}{Q_1}\right)^{2\gamma/(\gamma-1)}\right]. \quad (1)$$

Before integrating (1) it is convenient to introduce the non-dimensional variables

$$U = u/a_1, \qquad A = a/a_1, \qquad \xi = x/a_1 t_c, \qquad \tau = t/t_c,$$

where $t_c = 2a_1/(\gamma+1)b$ and b is the initial acceleration of the wall. The reason for selecting this particular form of t_c as a reference time will become apparent later. In terms of these variables (1) becomes

$$\frac{dU_w}{d\tau} = \frac{2}{\gamma+1}\frac{p_1}{p_{e0}-p_1}\left[\frac{p_{e0}}{p_1}\left(\frac{P_2'-U_w}{P_2'}\right)^{2\gamma/(\gamma+1)} - \left(\frac{Q_1'+U_w}{Q_1'}\right)^{2\gamma/(\gamma+1)}\right]. \quad (2)$$

p_{e0}/p_1, P_2' are constants which can be determined from the shock equations. Because of the particular way in which the system is made non-dimensional, Q_1' is a constant equal to $2/(\gamma-1)$. Equation (2) can be integrated twice

with the boundary conditions $\xi = U_w = 0$ at $\tau = 0$ to determine the path of the wall. From this and the flow variables at the wall the transmitted and reflected shocks can be determined.

Consider first the transmitted shock. It starts at the point which defines the cusp at the beginning of the envelope of the positive characteristics. Courant & Freidrichs (1948) show that this cusp occurs at $\tau = 1$, $\xi = 1$. The shock is then determined as follows. Neglecting entropy changes, the equation of the positive characteristic fg (see figure 2) is

$$\xi - \xi_f = (\tau - \tau_f)(U_f + A_f).$$

This must hold at the shock, whence

$$\xi_g - \xi_f = (\tau_g - \tau_f)(U_f + A_f). \tag{3}$$

Also

$$d\xi_g/d\tau_g = M_{Sg}, \tag{4}$$

where M_{Sg} is the shock Mach number at g. Since U is constant along fg,

$$M_{Sg} = \left(\frac{\gamma+1}{4} U_f\right) + \left[1 + \left(\frac{\gamma+1}{4} U_f\right)^2\right]^{1/2} = F(U_f). \tag{5}$$

Since ξ_f, A_f, U_f are known functions of τ_f, (3) and (4) can be integrated to find the coordinates of the transmitted shock. The boundary conditions are $d\xi_g/d\tau_g = \xi_g = 1$ at $\tau_g = 1$.

Similarly, for the reflected shock,

$$\xi_h - \xi_e = (\tau_h - \tau_e)(U_e - A_e)$$

and

$$\frac{d\xi_h}{d\tau_h} = U_2 - A_2 M_{Sg} = U_2 - A_2 F\left(\frac{U_2 - U_e}{A_2}\right),$$

where F is defined by (5). The appropriate boundary conditions are

$$d\xi_h/d\tau_h = U_2 - A_2(M_{Sh})_{\tau=0}, \qquad \xi_h = 0 \quad \text{at } \tau_h = 0.$$

The equations for the wall and those for the transmitted and reflected shocks are easily integrated numerically. Analytical solutions for the paths followed by the wall and shocks can be obtained, however, since the speed of the wall is conveniently represented by the series

$$U_w = D_0 + D_1 e^{-k\tau} + D_2 e^{-2k\tau} + D_3 e^{-3k\tau} + \ldots, \tag{6}$$

where D_0, D_1, D_2, D_3, ... and k are constants. k is positive. The form of (6) is suggested by the fact that the solutions of (2) show the behaviour $U_w \to 0$ as $\tau \to 0$ and $U_w \to$ constant as $\tau \to \infty$, together with the fact that for a weak incident shock

$$U_w = C(1 - e^{-k_1\tau}),$$

where

$$C = \frac{\gamma-1}{2\gamma} \frac{(p_{e0} - p_1)P_2' Q_1'}{p_{e0} Q_1' + p_1 P_2'}, \qquad k_1 = \frac{4\gamma}{\gamma^2 - 1} \frac{p_{e0} Q_1' + p_1 P_2'}{(p_{e0} - p_1)P_2' Q_1'}.$$

The boundary conditions combined with the relations obtained by substituting (6) in (2) are sufficient to determine the constants in (6). For moderate Mach numbers of the incident shock, only a small number of terms are required, three or four being sufficient for a Mach number of 1·5. The wall path is then obtained by integrating (6). The procedure for

determining the paths of the transmitted and reflected shocks is more complicated and in general it is simpler to calculate such paths by numerical integration.

3. The asymptotic behaviour of the system

The asymptotic speed of the wall can be determined from (2). This equation indicates that as the speed of the wall increases the acceleration decreases and eventually becomes zero. The final strengths of the shocks can be obtained from the final speed of the wall, since the fluid behind the shocks will be moving at the same speed as the wall. However, the asymptotic behaviour of the system can be obtained exactly, and independently of the above analysis, by one of a number of physical arguments which are true for any strength of incident shock. Such an argument is as follows. For a given incident shock Mach number, the only fundamental length in the problem is $\rho_w r/\rho_1$, where ρ_w is the density of the wall material, r the thickness of wall and ρ_1 the density of the fluid initially in the channel ($a_1 t_c$ is simply a constant multiple of $\rho_w r/\rho_1$). The strength of the transmitted shock can then depend only on the distance parameter $\xi' = x\rho_1/\rho_w r$, and its asymptotic value is obtained when $\xi' \to \infty$. This shows that the same shock strength is obtained whether $x \to \infty$ or $\rho_w r \to 0$. The case $\rho_w r = 0$ corresponds to the flow without the wall present and it can therefore be concluded that as $x \to \infty$ the strength of the transmitted shock tends to the strength of the incident shock. The reflected shock eventually becomes vanishingly weak. Although the transmitted shock eventually attains the same strength as the incident shock it will not at a given instant of time have reached the position that the incident shock would have reached if it had not encountered the wall. When the quasi-steady state is attained there will be a constant displacement between the position of the transmitted shock and the position that the incident shock would have reached. An expression for the amount of the displacement can be found as follows.

Figure 3 (*a*) shows a piston moving in a channel of uniform cross-section. The piston is started impulsively from rest at time $t = 0$ and continues to move with a constant speed u_2. A shock is generated which moves away from the initial position of the piston face with a constant speed w until it encounters a movable wall situated sufficiently far ahead of the piston to ensure that no disturbance travels back to the piston. Figure 3 (*b*) illustrates the case in which no wall is encountered. An expression is sought for the final value of the displacement δ between the two shocks. It will be supposed that in (*a*) the transmitted shock has not quite attained the strength of the incident shock. Define for (*a*) a velocity u_2' such that

$$u_2' = \frac{\int_0^{L-\delta} \rho u \, dx + \rho_w r u_w}{(L\rho_2 - \delta\rho_1) + \rho_w r},$$

$(L\rho_2 - \delta\rho_1)$ being the mass of the fluid between the shock and the piston in (*a*). u_2' will be close to the linear mean velocity of the fluid between the

shock and the piston in (*a*). Since the pressure on the pistons in both cases is the same and constant, the momentum contained between the pistons and some control surface ahead of the shocks must, at any instant of time, be the same for both systems. Therefore

$$L\rho_2 u_2 = [(L\rho_2 - \delta\rho_1) + \rho_w r]u_2',$$

and so

$$\delta = \rho_w r/\rho_1 - L\rho_2(u_2 - u_2')/u_2'.$$

Put $u_2 - u_2' = \Delta u$, where $\Delta u/u_2 \ll 1$, and note that $L = (w - u_2)t$ and $(w - u_2)\rho_2 = w\rho_1$, where w is the speed of the incident shock and t is the time measured from the instant at which the piston commenced to move. Then

$$\delta = \rho_w r/\rho_1 - wt\Delta u/u_2. \tag{7}$$

Now suppose that $\Delta u = B/t^n$, where n is positive. Equation (7) shows that, if $n < 1$, $\delta \to -\infty$ as $t \to \infty$, which is clearly impossible. If $n = 1$, δ is independent of t and therefore independent of Δu. This is also impossible since $d\delta/dt$ is a function of Δu. Or, more simply, if Δu is not zero the shocks are not of equal strength and δ must change with time. Therefore $n > 1$ is the only case admissible. As $t \to \infty$, $\delta \to \rho_w r/\rho_1$.

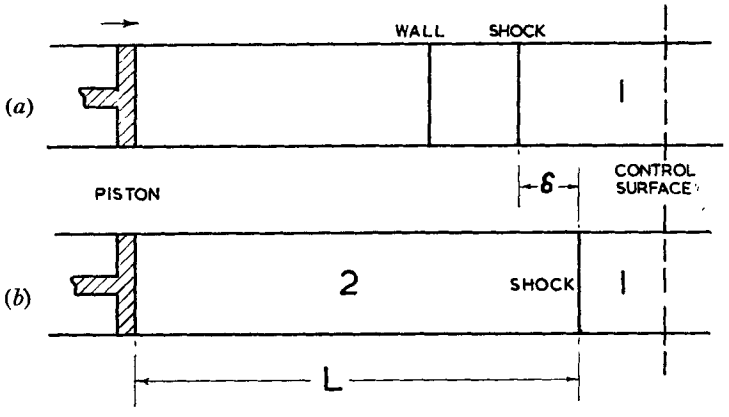

Figure 3. The displacement of the transmitted shock from the position that the incident shock would have attained if it had not encountered the wall.

The fact that the transmitted shock must eventually become equal in strength to the incident shock provides a useful check on the approximate theory. It also gives an indication of how p_{e0}/p_1, which appears in (2), should be determined. Consistently with the approximate theory, p_{e0}/p_1 may be calculated assuming isentropic compression through the reflected shock, or alternatively, the shock relations may be used to determine the exact value of p_{e0}/p_1. On first thoughts it might appear that there would be some advantage in having the initial pressure difference across the wall correct. Figure 4 shows plots of the ratio $(U_w \text{ approx.})_{\tau\to\infty}/(U_w \text{ true})_{\tau\to\infty}$ against incident shock Mach number. The upper curve is obtained using the 'isentropic' value of p_{e0}/p_1, whereas the lower curve is determined with the exact value of p_{e0}/p_1. The approximate theory appears to be

best if the 'isentropic' value of p_{e0}/p_1 is used, although the additional error introduced by using the exact value of p_{e0}/p_1 is not great. Figure 4 also indicates that the approximate theory predicts $(U_w)_{\tau\to\infty}$ fairly accurately even when the incident shock Mach number is far from unity.

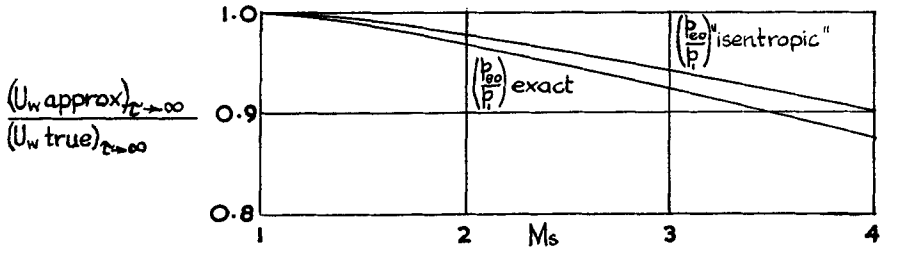

Figure 4. Error in the approximate theory.

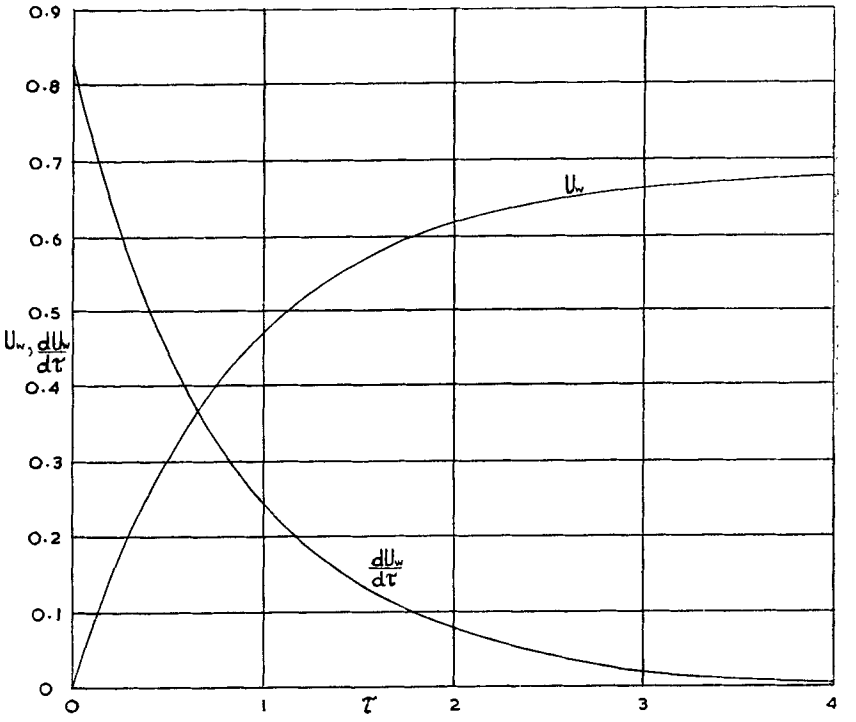

Figure 5. Variation with time of the wall speed and the wall acceleration.

The behaviour of the wall, the transmitted shock and the reflected shock have been computed for an incident shock Mach number of 1·500. Figure 4 shows that at this incident shock Mach number the final speed of the wall as predicted by the approximate theory differs from the true final speed by about 1%. The computed results are summarized in figures 5, 6 and 10. In figure 10, where the experimental results are compared with the theory, the paths of the wall, the transmitted shock and the reflected shock are

shown. Figure 5 shows the variation with time of wall acceleration and of wall speed. Figure 6 shows how the strengths of the transmitted and reflected shocks vary as they propagate, together with the asymptotic values of $M_S - 1$. The fact that these asymptotic values differ by only small amounts

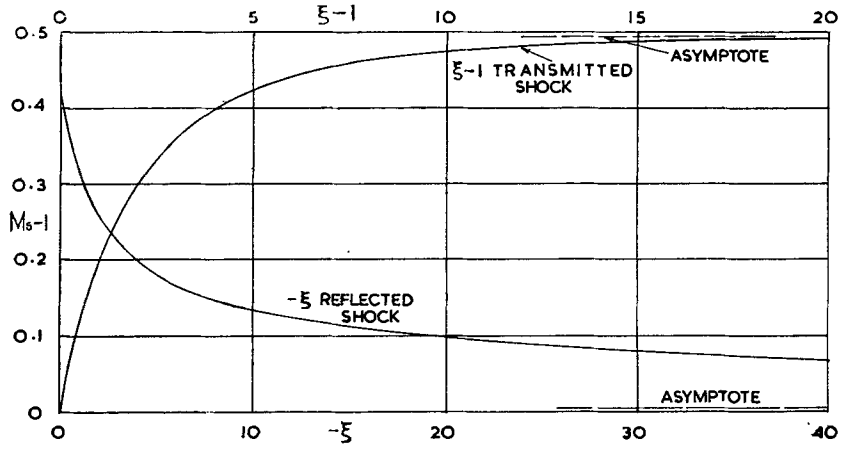

Figure 6. Variation in the strength of the transmitted and reflected shocks.

from 0·500 and 0 respectively is a further indication that the error in the approximate theory for an incident shock Mach number of 1·500 is small.

4. The shock tube

The shock tube at the Mechanics of Fluids Laboratory is of rectangular cross-section 5·785 in. deep and 1·500 in. wide; it is 13 ft. 6 in. long and closed at one end. The diaphragm is 12 ft. from the closed end and the high pressure section is maintained at atmospheric pressure. The required pressure ratio across the diaphragm is achieved by evacuating the low pressure section of the shock tube. The shock speed is measured by timing the passage of the shock between two schlieren light screens placed 1 ft. apart. Investigations are usually made by schlieren spark photography, and photographs, only one per run, can be taken at known pre-set delays after the shock passes the second light screen. The use of the shock tube is limited to a shock Mach number below about 1·9, because above this the density in the shock tube becomes too low for the light screens to function. A general description of the tube together with its instrumentation is given by Lapworth (1954).

5. Experiments

The object of the experimental study was to determine the motions of the wall, the transmitted shock and the reflected shock by taking photographs of the interaction at various known time intervals after the incident shock had passed the second light screen.

The experimental conditions were chosen to make the scale of the experiment suit the size of the shock tube ($a_1 t_c \doteqdot 4$ in. or $b \doteqdot 3 \times 10^6$ ft./sec^2).

For an incident shock Mach number of 1·500 a cellulose acetate sheet 0·0017 in. thick gave $a_1 t_c = 4{\cdot}025$ in. and $b = 3{\cdot}100 \times 10^6$ ft./sec^2. Some experiments were carried out with walls of 0·0010 in. and 0·0030 in. thick cellulose acetate, using the same incident shock Mach number, to check that the results (in non-dimensional form) were, as the theory suggested, independent of the mass of the wall.

Owing to the difficulty of mounting the wall in the full cross-section of the shock tube it was decided to use a channel of reduced cross-section, obtained by inserting liners in the working section. This scheme also had the advantage that the holding device for the wall could be shifted simply by moving the liners along the shock tube. The reduced channel was 2·830 in. deep and 1·500 in. wide.

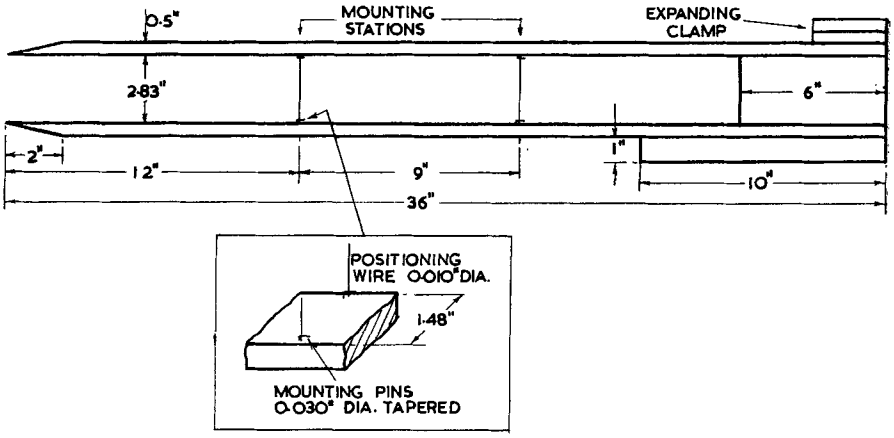

Figure 7. Liners, together with details of mounting pins and positioning wires.

Lack of stiffness made it necessary to support the wall until it was struck by the shock. Support was provided by impaling each corner of the wall on a slender pin pointing in the direction in which the wall was to move. Figure 7 is a diagram of the liners showing details of the mounting pins. The vertical wires alongside the pins were provided so that the wall could be placed in the same position, against the wires, for each run. In mounting the wall it was required that the wall should as nearly as possible fill the cross-section of the working channel and also that it should be as plane as possible. Meeting these requirements was the most difficult part of the experiment. Figure 8 shows the device that was eventually used in mounting the sheet cellulose acetate. Strips of the wall material 1·500 in. wide were stretched and accurately held on the device by the movable clamp. The device was then carefully placed between the liners and the strip of wall material accurately positioned on the pins. A sharp knife was used to cut the wall to size in position. The wall was left with some wrinkles when the mounting device was removed, but when the shock tube was closed and the

pressure reduced the cellulose acetate dried slightly, shrinking in the process, and was left stretched plane on the pins*.

Experiments were carried out to measure the loss of mass of the cellulose acetate due to drying which was found to be of the order of 1%. Account was taken of this loss of mass.

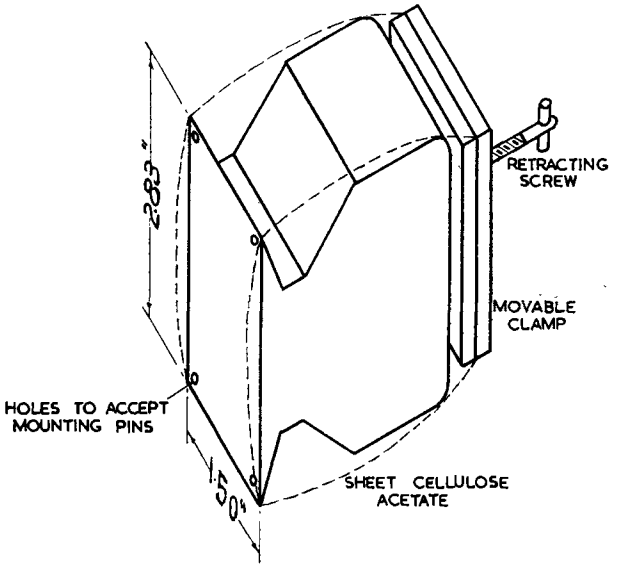

Figure 8. Device for positioning the wall.

Measurements of the photographic negatives, 0·6 full size, were made with a travelling microscope accurate to $\pm 0{\cdot}0005$ in. All measurements were made on the centre line of the working channel. The pressure in the shock tube was measured with a mercury manometer accurate to $\pm 0{\cdot}2$ mm Hg. The ambient temperature was measured with a mercury thermometer accurate to $\pm 0{\cdot}1^\circ$ C. Throughout all experiments an endeavour was made to keep the variations of incident shock Mach number to within 1% and this was nearly always achieved.

6. Experimental results and discussions

Figure 9 (plate 1) shows the wall in several positions after it has been struck by the shock. In figure 9(*a*) the mounting pins, the positioning wires and the wall are seen, while in the others only the wall appears. During the early stages of its motion the wall remains very flat, but as it progresses away from its initial position the edges are observed to lag behind the main body of the wall. The curling of the edges increases as the motion of the wall proceeds, although the extent of the curling is not

* The artifice of allowing material like cellulose acetate to dry in order to produce a taut diaphragm is well known domestically in the preparation of covers for jam-jars.

considerable until the wall has moved some distance. At $x = 3{\cdot}583$ in., figure 9(*d*), the shape of the wall is still a good approximation to the ideal plane moving wall, but at $x = 6{\cdot}726$ in., figure 9(*e*), this is no longer the case since the wall has become distinctly curved. When the wall reaches $x = 6{\cdot}726$ in. it has attained a speed which is about 90% of its final speed, and from then on its speed is changing only slowly so that most of the interesting part of the wall path has already been covered. It should be remembered that the plates showing the wall are photographs of different walls at the various distances and not photographs of the same wall at these distances. No attempt should therefore be made to follow too closely the distortions of the wall from one photograph to the next for it may occur that photographs of different walls in the same position are different in detail. The curling of the edges of the wall needs some explanation.

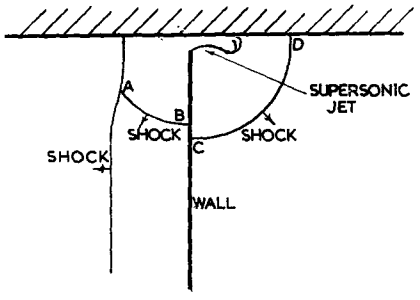

Figure 10. Diagrammatic sketch of the shock wave pattern near a gap at the edge of the wall from which a shock wave is reflected.

It appears that the curling of the wall edges results mainly from leakage past the edges of the wall. Figure 13 (plate 2) shows the interaction of a shock with a movable wall in which large gaps have intentionally been left at the top and bottom edges of the wall and figure 10 is a diagrammatic sketch of the interaction in the neighbourhood of a gap. Part only of the shock AB is seen in figure 13 (*a*) since it is very weak and since the schlieren photograph was taken with the knife edge perpendicular to the direction of flow. Approximate analysis of the normal reflection of a shock at a wall with a slit in it, by Whitham's (1957) theory, together with the results of an experimental investigation by the author, suggest that the shocks AB and CD are too weak at the wall to be responsible for the observed curling. Modification of the pressure forces near the edges of the wall by the flow past the edges is thought to be the main cause of the curling. The fluid approaches the gap, accelerates, passes through the gap, separation occurs at the edge of the wall and a small supersonic jet forms. The decrease in pressure of the fluid approaching the gap reduces the pressure difference across the wall in the neighbourhood of the gap, causing the edges to lag behind the main body of the wall. Provided that the gaps are small and the curling slight, leakage should have only a small effect on the motion of the wall as a whole.

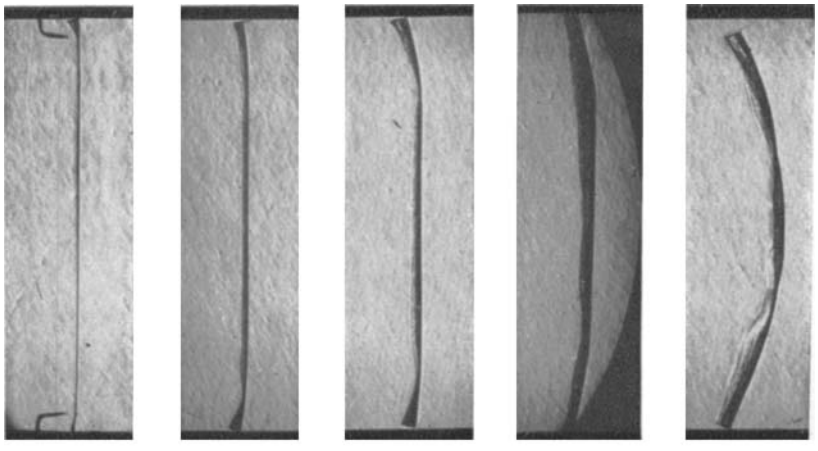

(*a*) (*b*) (*c*) (*d*) (*e*)

Figure 9. The moving wall in several positions after being struck by the shock wave.

(*a*) $\tau = 0{\cdot}300$, $\xi = 0{\cdot}034$, $x = 0{\cdot}144$ in. ;
(*b*) $\tau = 0{\cdot}947$, $\xi = 0{\cdot}250$, $x = 1{\cdot}035$ in. ;
(*c*) $\tau = 1{\cdot}751$, $\xi = 0{\cdot}644$, $x = 2{\cdot}684$ in. ;
(*d*) $\tau = 2{\cdot}076$, $\xi = 0{\cdot}859$, $x = 3{\cdot}583$ in. ;
(*e*) $\tau = 3{\cdot}280$, $\xi = 1{\cdot}659$, $x = 6{\cdot}726$ in.

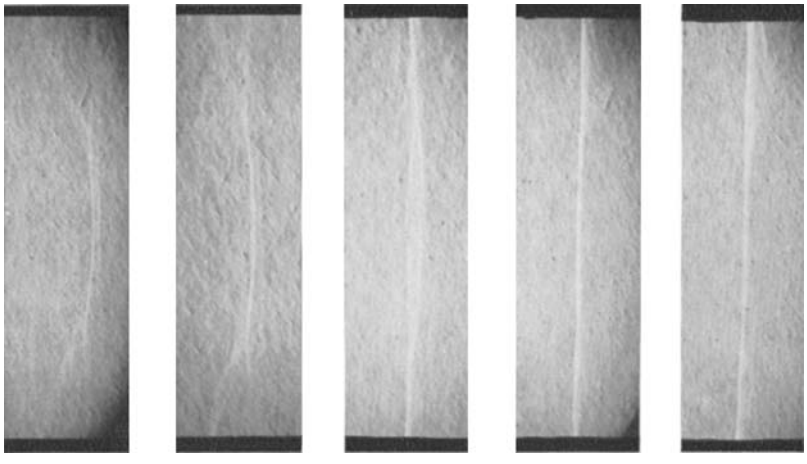

(*a*) (*b*) (*c*) (*d*) (*e*)

Figure 11. The transmitted shock in various stages of formation.

(*a*) $\tau = 1{\cdot}140$, $\xi = 1{\cdot}242$, $x = 5{\cdot}122$ in. ;
(*b*) $\tau = 1{\cdot}275$, $\xi = 1{\cdot}396$, $x = 5{\cdot}678$ in. ;
(*c*) $\tau = 1{\cdot}670$, $\xi = 1{\cdot}847$, $x = 7{\cdot}627$ in. ;
(*d*) $\tau = 2{\cdot}520$, $\xi = 2{\cdot}897$, $x = 11{\cdot}987$ in. ;
(*e*) $\tau = 3{\cdot}228$, $\xi = 3{\cdot}983$, $x = 16{\cdot}183$ in.

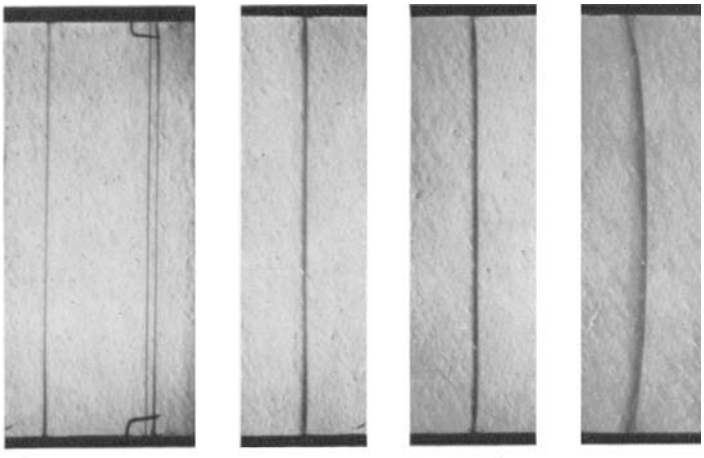

(*a*) (*b*) (*c*) (*d*)

Figure 12. The reflected shock at several distances from the initial position of the wall.
(*a*) $\tau = 0{\cdot}178$, $\xi = -0{\cdot}170$, $x = -\ 0{\cdot}685$ in. ;
(*b*) $\tau = 0{\cdot}358$, $\xi = -0{\cdot}325$, $x = -\ 1{\cdot}312$ in. ;
(*c*) $\tau = 0{\cdot}688$, $\xi = -0{\cdot}611$, $x = -\ 2{\cdot}474$ in. ;
(*d*) $\tau = 3{\cdot}388$, $\xi = -2{\cdot}573$, $x = -10{\cdot}494$ in.

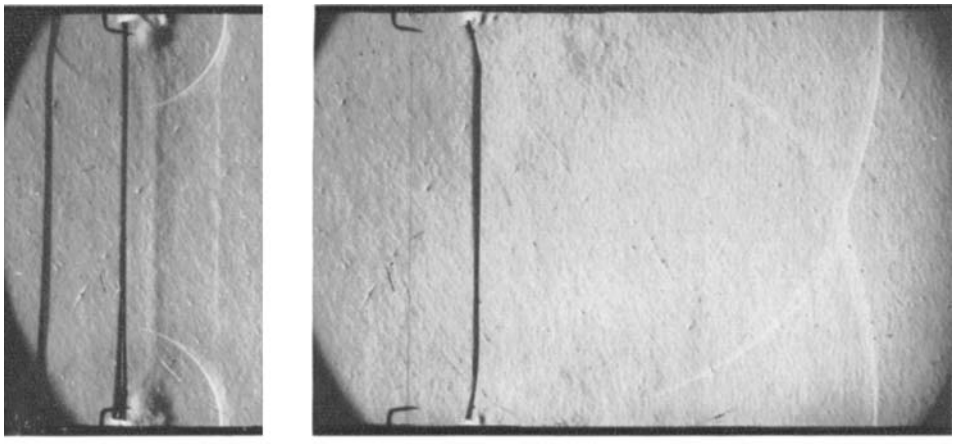

(*a*) (*b*)

Figure 13. Two stages in the motion following the impact of a shock wave on a movable wall along the top and bottom edges of which large gaps have been left.

Figure 11 (plate 1) shows the transmitted shock at various stages during its formation. Figures 11 (*a*) and (*b*) show that during its initial stages the transmitted shock is far from plane and its ends are forked. This is due to the fact that the transmitted shock is composed not only of compression waves coming from the accelerating wall but also of weak shocks which originate at the gaps around the edges of the wall. The transmitted shock is thus the result of the interaction of four approximately cylindrical shocks, some of which may be stronger than others, and the compression waves coming from the accelerating wall. The nature of the shocks coming from the gaps and their interaction are shown in figure 13 (plate 2). Figures 11 (*c*), (*d*) and (*e*) (plate 1) show that as the transmitted shock propagates it soon takes up the stable plane form for a shock travelling in a straight duct of uniform cross-section.

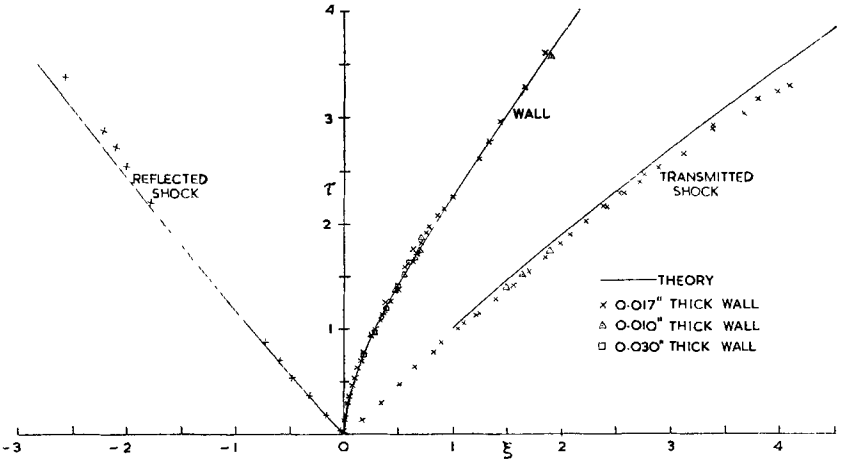

Figure 14. Comparison of the theoretical and experimental results.

Figure 12 (plate 2) shows the reflected shock at several distances from the point at which the incident shock struck the wall. In figure 12 (*a*) the mounting pins, the positioning wires and the reflected shock are seen while in the others only the reflected shock appears. The reflected shock is plane to start with, but as it moves away from the initial position of the wall it becomes curved at the channel walls and woolly in appearance. The curving and the woolly appearance are due to the growth of the boundary layer on the channel walls. In figure 12 (*d*) the boundary layer on the channel walls appears to be relatively thick.

Figure 14 compares the theoretical and experimental results. Before discussing the comparison in detail it would be as well to consider the relative sizes of the errors in the theory and those in the experimental technique. It has already been stated that for an incident shock Mach number of 1·500, the approximate theory predicts the final speed of the wall with an error of the order of 1%. Figure 6 indicates that the final

Mach numbers of the transmitted and reflected shocks are also given with an error of approximately 1%. If it is assumed that the approximate theory gives the wall speed and the shock Mach numbers correct to 1% for all times, then the displacements of the wall, the transmitted shock and the reflected shock will also be given with an error of only 1%. Since the errors in the experimental technique are about 1% the errors in the approximate theory are not thought to be significant in the comparison of the theoretical and experimental results.

Referring again to figure 14, it will be seen that there is good agreement between the theoretically determined curve for the path followed by the wall and the experimentally determined points. It is also apparent that the results are, as expected, independent of the mass of the wall. The experimental points for the reflected shock agree well with the theoretical curve for the initial part of the shock path, but for larger times the shock lags behind the position predicted by theory. Part at least of this lag is due to leakage past the edges of the wall and leakage past the sides of the liners, which were made 0·20 in. narrower than the shock tube to avoid damaging the working section windows. The experimental results for the transmitted shock show two distinct departures from the theoretically determined shock. In the first place, a shock appears in the region $0 < \xi < 1$ where theory predicts none and, secondly, the experimental points appear consistently ahead of the theoretically determined shock. The appearance of shocks in the region $0 < \xi < 1$ is due simply to shocks getting past the edges of the wall. The displacement is probably due to leakage past the edges of the wall and to leakage past the sides of the liners; the displacement at $\xi = 1$, $\tau = 1$, where, in theory, the transmitted shock wave should just begin to form, is mainly due to the former type of leakage. It is difficult to give a detailed analysis of the effect of leakage, but a simple model can be imagined which will probably yield an answer of the correct order of magnitude. Assume that the gap is uniformly distributed over the wall or, in other words, that the wall is porous. Further assume that the leakage through the wall and the wall acceleration remain constant for a short time. The contact surface, which separates the gas which has passed through the wall and that which has not, moves away from the wall with a constant speed, and so the transmitted shock can be imagined as resulting from the motion of a piston which is impulsively given a small speed and then accelerates with the acceleration of the wall. The transmitted shock starts at $\xi = 0$, $\tau = 0$, and by using Friedrichs' (1948) theory, the position of the transmitted shock at $\tau = 1$ can be found for a given initial velocity of the contact surface. Or, given the position of the shock at $\tau = 1$, the initial velocity of the contact surface can be found. From this, assuming isentropic expansion through the wall, the leakage area of the wall can be determined. According to this argument the observed displacement was consistent with a leakage area equivalent to a gap of 0·005 in. along all edges of the wall. This appears to be of the correct order of magnitude, bearing in mind the difficulty of arranging the flimsy wall-material, 0·0017 in.

thick, to fill completely the cross-section of the tube and the gap of 0·01 in. between the liners and the walls of the shock tube.

The author wishes to acknowledge much helpful advice and constructive criticism given him by Dr N. H. Johannesen and Professor P. R. Owen. He is also grateful to the Defence Scientific Corps, Royal New Zealand Air Force, for making his period of study at Manchester University possible.

References

COURANT, R. & FRIEDRICHS, K. O. 1948 *Supersonic Flow and Shock Waves.* New York : Interscience.

FRIEDRICHS, K. O. 1948 Formation and decay of shock waves, *Comm. Pure Appl. Math.* **1**, 211.

LAPWORTH, K. C. 1954 M.Sc. Thesis, Manchester University. (Precis available in *Aero. Res. Counc., Lond., Rep.* no. 17328.)

PILLOW, A. F. 1949 The formation and growth of shock waves in the one-dimensional motion of a gas, *Proc. Camb. Phil. Soc.* **45**, 558.

PILLOW, A. F. & LEVEY, H. C. 1947 The formation and growth of shock waves in the one-dimensional motion of a gas, *Aus. Counc. Sci. Indus. Res., Div. Aero. Rep.*, no. A47.

RUDINGER, G. 1955 *Wave Diagrams for Non-steady Flow in Ducts.* Princeton : Van Nostrand.

WHITHAM, G. B. 1957 A new approach to problems of shock dynamics, *J. Fluid Mech.* **2**, 145.